J Cardiovasc Imaging. 2022 Jul;30(3):169-180
https://doi.org/10.4250/jcvi.2021.0189
pISSN 2586-7210·eISSN 2586-7296

Journal of Cardiovascular Imaging JCVI

Original Article

Check for updates

Evaluation of Non-infarct-Related Arteries Using C-11 Acetate PET in STEMI With Multivessel Disease

Sang-Geon Cho, MD, PhD, FANMB[1], Minchul Kim, MD, PhD[2], Seung Hun Lee, MD, PhD[2], Ki Seong Park, MD[1], Jahae Kim, MD, PhD, FANMB[1], Jang Bae Moon, MD, PhD[1], and Ho-Chun Song, MD, PhD[1]

[1]Department of Nuclear Medicine, Chonnam National University Hospital, Gwangju, Korea
[2]Department of Cardiology, Chonnam National University Hospital, Gwangju, Korea

OPEN ACCESS

Received: Nov 30, 2021
Revised: Feb 14, 2022
Accepted: Feb 17, 2022
Published online: Mar 3, 2022

Address for Correspondence:
Ho-Chun Song, MD, PhD
Department of Nuclear Medicine, Chonnam National University Hospital, 42, Jebong-ro, Dong-gu, Gwangju 61469, Korea.
Email: songhc@jnu.ac.kr

ORCID iDs
Sang-Geon Cho
https://orcid.org/0000-0002-1373-1887
Minchul Kim
https://orcid.org/0000-0001-6026-1702
Seung Hun Lee
https://orcid.org/0000-0002-2337-7826
Ki Seong Park
https://orcid.org/0000-0003-3610-1957
Jahae Kim
https://orcid.org/0000-0003-4077-7722
Jang Bae Moon
https://orcid.org/0000-0001-7183-2427
Ho-Chun Song
https://orcid.org/0000-0002-6407-8160

Funding
This research was supported from the Korean Cardiac Research Foundation (Grant No. 201803-02).

ABSTRACT

BACKGROUND: We analyzed whether C-11 acetate positron emission tomography (PET) can be used for the evaluation of non-infarct-related artery (NIRA) in patients with ST-elevation myocardial infarction (STEMI) and multivessel disease.
METHODS: We prospectively enrolled 31 patients with STEMI and at least one NIRA stenosis (diameter stenosis [DS] ≥ 50%). C-11 acetate PET was performed after successful revascularization for the infarct-related artery (IRA). Myocardial blood flow (MBF) and oxidative metabolism (k_{mono}) were measured and compared between NIRA vs. IRA, stenotic (DS ≥ 50%) vs. non-stenotic (DS < 50%) NIRAs, and NIRAs with significant stenosis (DS ≥ 70% or fractional flow reserve [FFR] ≤ 0.80) vs. those without (neither DS ≥ 70% nor FFR ≤ 0.80). The correlations between PET and angiographic parameters were also analyzed.
RESULTS: MBF and k_{mono} were significantly higher in NIRAs than those in IRAs. Stenotic NIRAs showed significantly reduced stress MBF, myocardial flow reserve (MFR), relative flow reserve (RFR) (0.72 ± 0.12 vs. 0.82 ± 0.14; p = 0.001), and stress k_{mono}, as compared to those in non-stenotic NIRAs. NIRAs with significant stenosis had significantly lower stress MBF, MFR, and RFR (0.70 ± 0.10 vs. 0.80 ± 0.14; p = 0.001). RFR showed the best, but modest linear correlation with DS of NIRA stenosis (r = −0.429, p = 0.001). RFR > 0.81 could effectively exclude the presence of significant NIRA stenosis.
CONCLUSIONS: C-11 acetate PET could be a feasible alternative noninvasive modality in patients with STEMI and multivessel disease, by excluding the presence of significant NIRA stenosis.

Keywords: ST elevation myocardial infarction; Positron emission tomography; Myocardial perfusion imaging; Oxygen consumption

INTRODUCTION

A half of patients with ST-elevation myocardial infarction (STEMI) have multivessel disease.[1] The presence of multivessel disease is associated with an increased risk of cardiac events even after successful acute management.[2] To reduce the risk of future cardiac events, the current guidelines recommend staged percutaneous coronary intervention (PCI) for non-infarct-related artery (NIRA) stenosis, in addition to primary PCI for the infarct-related artery (IRA), in selected patients who are hemodynamically stable.[3]

Journal of Cardiovascular Imaging JCVI

Conflict of Interest
The authors have no financial conflicts of interest.

Author Contributions
Conceptualization: Cho SG; Data curation: Cho SG, Kim M, Lee SH; Formal analysis: Cho SG, Park KS; Funding acquisition: Cho SG; Investigation: Cho SG, Kim M, Lee SH, Moon JB; Methodology: Cho SG, Park KS, Kim J, Moon JB; Project administration: Cho SG, Song HC; Resources: Song HC; Software: Cho SG, Park KS, Moon JB; Supervision: Kim J, Song HC; Validation: Kim J, Song HC; Visualization: Cho SG; Writing - original draft: Cho SG; Writing - review & editing: Kim M, Lee SH, Kim J, Song HC.

However, additional invasive procedure may prolong hospital stay and increase the risk of periprocedural complications including allergic reactions, further myocardial infarction, arrhythmia, stroke, vascular dissection and perforation, infection, contrast nephropathy and bleeding.[4] If a noninvasive imaging study appropriately determines the severity of NIRA stenosis after primary PCI, the need for prolonged, unnecessary invasive procedures and related complications can be reduced. Also, an imaging study performed in a more stabilized state after primary PCI may improve the assessment of NIRA stenosis, which can be erroneous during the index procedure due to physiologic vasoconstriction, blunted hyperemic response, and microvascular compression following acute myocardial ischemic insult.[5][6]

C-11 acetate positron emission tomography (PET) can simultaneously quantify myocardial blood flow (MBF) and oxidative metabolism, both of which are decreased by ischemia,[7] in a noninvasive manner. It could provide information on the global ischemic burden and energy efficiency at the level of the myocardium.[8] However, despite the technical and clinical validations in ischemic heart failure, hypertrophic cardiomyopathy, alcoholic cardiomyopathy, and diabetes-related myocardial changes,[9-12] its role has not been explored in the assessment of NIRA stenosis in patients with STEMI and multivessel disease yet. Thus, in this prospective proof-of-concept study, we evaluated whether C-11 acetate PET study is clinically feasible option for the assessment of NIRA in patients with STEMI and multivessel disease, based on the quantitative measurements of MBF and oxidative metabolism.

METHODS

Patients

We prospectively enrolled patients eligible for the present study from October 2020 to July 2021. Eligibility criteria included 1) STEMI with successful primary PCI for the IRA with 12 hours of symptom onset; 2) diameter stenosis (DS) ≥ 50% in NIRA with ≥ 2.5 mm diameter by visual estimation; 3) planned for a staged PCI. Exclusion criteria included 1) immediate multivessel PCI; 2) hemodynamically unstable patients; 3) unprotected left main coronary artery disease with DS ≥ 50%; 4) chronic total occlusion involving NIRA; 5) history of prior myocardial infarction or bypass surgery; 6) systolic heart failure with ejection fraction < 40% following STEMI; 7) contraindication to adenosine vasodilator stress.

All patients were informed of the study purpose, design, and related procedures and asked to participate in the prospective study after primary PCI during admission. Those who agreed to participate signed the informed consent. The prospective enrollment and data analyses were approved by the Chonnam National University Hospital Institutional Review Board (CNUH-2018-267).

Coronary angiography (CAG) and invasive parameters

CAG was performed following the standard procedures as previously described.[13] Fractional flow reserve (FFR) was measured for NIRAs with intermediate stenosis (50–70%) by visual estimation during the staged CAG. A NIRA stenosis with either DS ≥ 70% or FFR ≤ 0.80 was considered eligible for staged PCI.[14] DS was quantified by dividing the minimal diameter by the reference diameters obtained from the proximal and distal reference segments.

NIRAs were classified into binary groups according to the presence and severity of stenosis. NIRAs with DS ≥ 50% were regarded as stenotic, while the others were regarded as non-

https://doi.org/10.4250/jcvi.2021.0189

Journal of Cardiovascular Imaging JCVI

stenotic. Significant stenosis was defined as either DS ≥ 70% or FFR ≤ 0.80[14]; NIRAs were classified as those with and without significant stenosis.

Acquisition of C-11 acetate PET

After the primary PCI, C-11 acetate PET was performed prior to the staged CAG. A dedicated PET/computed tomography (CT) scanner (Discovery STE; GE Healthcare, Chicago, IL, USA) was used, based on a one-day rest-stress protocol with adenosine stress. Patients were instructed to fast at least for 4 hours prior to image acquisition while avoiding caffeine-containing foods or beverages at least for 2 days, and vasodilator medication on the day of image acquisition.

First, a low-dose CT was performed for the chest including the whole heart for attenuation correction. Then, 222–296 MBq of C-11 acetate was intravenously administered as a bolus using an automated contrast media injector (Optivantage DH®; Mallinckrodt, Hazelwood, MO, USA). Dynamic rest images were acquired for 20 minutes in list mode, which were to be split into 28 frames composed of 6 frames × 10 seconds, 4 frames × 15 seconds, and 18 frames × 60 seconds.[15] Ten minutes after the rest image acquisition, which correlates to 30 minutes following the first injection of C-11 acetate, adenosine was intravenously infused into the opposite arm at 140 ug/kg/min for 6 minutes. Measuring the patient's heart rate and blood pressure, the same dose of C-11 acetate was intravenously administered at 3 minutes. The stress images were acquired based on the same protocol as described above.

For effective image acquisition in clinical practice, C-11 acetate PET study was performed based on a single production of radioisotope which yielded a median of 5,180 MBq of C-11 acetate.

Quantification of MBF and oxidative metabolism

A nuclear cardiology expert with > 10 years of experience, who was blinded to the patients' characteristics and invasive measures, analyzed the PET images. As C-11 acetate is taken up by the myocardium and washed out progressively, the summed myocardial activity from the 10th through the 25th frames was selectively used for base-to-apex cardiac axis allocation and standard positioning, because of its optimal myocardium-to-background contrast. The epi- and endomyocardial borders were defined on short-axis images to delineate the volume of interest for the left ventricular myocardium. Input functions were acquired from the blood pool of the left and right ventricles with caution to avoid spillover from the myocardial activity (**Figure 1**).

MBF, the absolute amount of perfusion a specific mass of myocardium receives per minute, was quantified using a 1-tissue compartment model for C-11 acetate as previously described.[16] Myocardial oxidative metabolism was represented by k_{mono}, which is derived by monoexponential curve fitting of the washout phase of the C-11 acetate time-activity curve, along with metabolite correction.[15] As the initial decline in myocardial activity differed between segments and individuals, k_{mono} was quantified invariably using image frames beyond 2 minutes in all patients. The PET image analyses were conducted using a dedicated software package (Carimas™; Turku PET Centre, Turku, Finland) (**Figure 1**).

MBF and k_{mono} were measured for the respective coronary territories, as well as the entire left ventricle (LV), based on the standardized 17-segment model (**Supplementary Figure 1**).[17] Myocardial flow reserve (MFR) was defined as the ratio of stress to resting MBF. Relative flow reserve (RFR) was defined as the ratio of stress MBF of a specific coronary territory to the highest segmental MBF throughout the entire LV.[18] The ratio of stress to rest k_{mono} was

https://doi.org/10.4250/jcvi.2021.0189

Journal of Cardiovascular Imaging JCVI

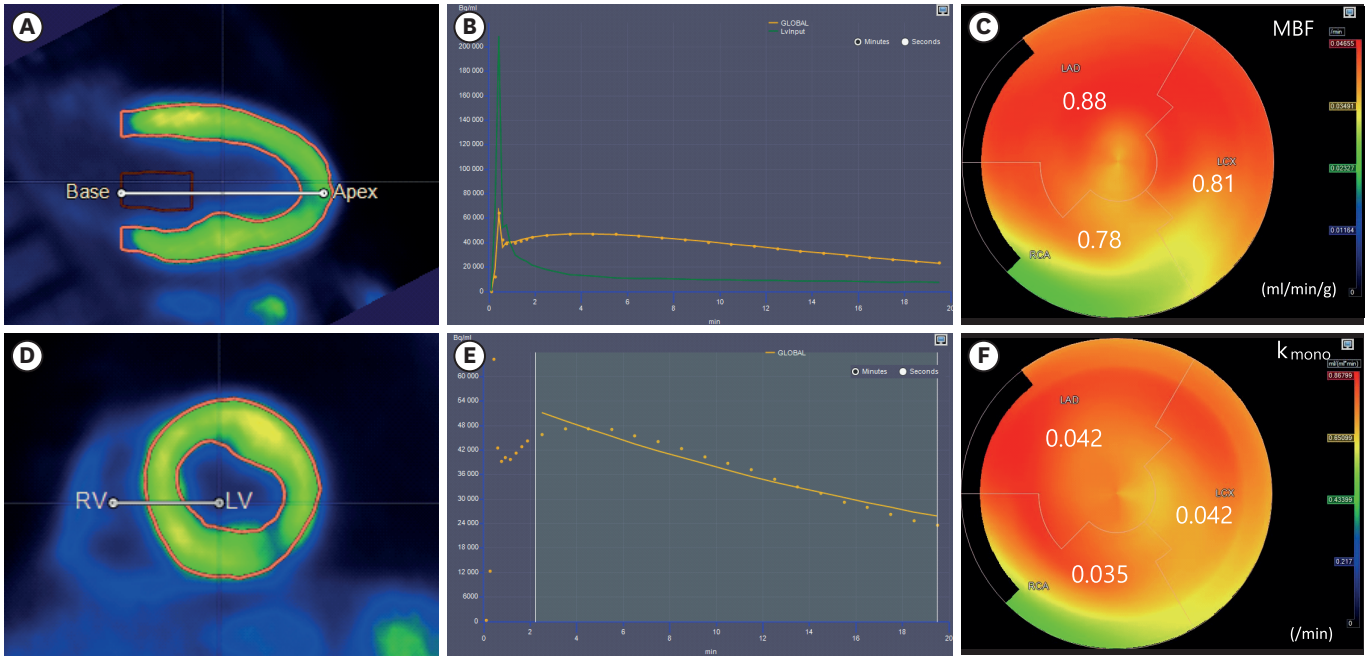

Figure 1. Analyses of C-11 acetate PET for quantification of MBF and oxidative metabolism in a 65-year-old man with STEMI in the RCA territory. For the delineation of the LV myocardium and blood pool, the summed images from the 10th through the 25th frames were selectively used for cardiac axis allocation and standard positioning (A, D). The time-activity curve is obtained from the LV blood pool and LV myocardium, from which both MBF (B, C) and k_{mono} (E, F) can be calculated. The image frames beyond 2 minutes (colored area, E) are used for k_{mono} calculation, because of the difference in the initial decline in myocardial C-11 acetate activity between segments and individuals.
RV, right ventricle; LV, left ventricle; MBF, myocardial blood flow; PET, positron emission tomography; RCA, right coronary artery; STEMI, ST-elevation myocardial infarction; LAD, left anterior descending artery; LCx, left circumflex artery.

also calculated, which was referred to as oxidative metabolism reserve. For a combined assessment of perfusion and oxidative metabolism, we calculated the product of MBF and k_{mono} (MBF*k_{mono}). By the definitions of MBF and k_{mono}, MBF*k_{mono} indicates the amount of perfusion, which provides the correlating amount of oxygen, that undergoes oxidative metabolism per minute for a specific mass of myocardium. The PET results were also blinded to the clinical and interventional cardiologists participating in patient management.

Statistical analyses

Continuous variables were presented as mean ± standard deviation or median (range) according to the results of Shapiro-Wilk normality test; categorical variables were presented as number (%). The PET parameters were compared between NIRA vs. IRA using either Student's t-test or Mann-Whitney U test according to the data distribution. These values were also compared between NIRAs with and without significant stenosis, and between normal and abnormal NIRAs. The correlations between DS, FFR, and echocardiographic parameters vs. PET indices were evaluated by Pearson's or Spearman's correlation analysis. Receiver operating characteristics curve analysis was performed to obtain optimal thresholds of the PET parameters for detecting stenoses in NIRAs. R v4.0.2 (R Foundation for Statistical Computing, Vienna, Austria) was used for the statistical analyses. A $p < 0.05$ was considered statistically significant.

https://doi.org/10.4250/jcvi.2021.0189

Journal of Cardiovascular Imaging JCVI

RESULTS

Baseline characteristics

The initial screening found 43 patients eligible for the present study, while 12 of them were excluded for refusal to participate (n = 6), hemodynamic instability after primary PCI (n = 1), unprotected left main disease (n = 1), planned for bypass surgery (n = 1), failed C-11 acetate production (n = 1), and chronic total occlusion in NIRA (n = 1). The final study participants included 24 males and 7 females with an overall median age of 67 (41–75) years. The most common IRA was the right coronary artery, followed by the left anterior descending artery and left circumflex artery. The interval between primary PCI for STEMI and PET was 3 (1–5) days, while that between PET and staged CAG was 1 (0–4) days. Among the 62 NIRAs, 42 (62%) were stenotic. FFR was measured in 25 NIRAs; 18 (29%) had significant stenosis. More detailed baseline characteristics are listed in **Table 1**.

Table 1. Baseline characteristics

Characteristics	Value
Age (years)	65 (42, 87)
Sex	
Male	24 (77)
Female	7 (23)
Diabetes	6 (19)
Hypertension	14 (45)
Dyslipidemia	25 (81)
Obesity	11 (37)
Current smoking	10 (32)
Ex-smoking	5 (16)
Troponin-I (ng/mL)	
Initial	0.30 (0.02, 19.65)
Peak	11.11 (0.66, 125.00)
Echocardiography	
LVEF (%)	59.1 (49.7, 69.8)
LVEDV (mL)	122.0 (64.4, 218.8)
LVESV (mL)	47.3 (27.8, 107.8)
GLPSS (%)	−12.8 (−5.3, −19.8)
Diastolic dysfunction	
Grade 1	3 (10)
Grade 2	26 (84)
Grade 3	2 (6)
E/A	0.81 (0.49, 1.55)
E/e'	11.00 (1.17, 29.00)
Interval between primary PCI and PET (days)	3 (1, 5)
Interval between PET and staged CAG (days)	1 (0, 4)
IRA	
LAD	7 (23)
LCx	5 (16)
RCA	19 (61)
2VD	20 (65)
3VD	11 (35)
DS (%), NIRA (n = 42)	67 (52, 97)
FFR, NIRA (n = 25)	0.87 (0.65, 0.98)

Data are presented as mean ± standard deviation or median (range) for continuous variables and number (%) for categorical variables.
CAG, coronary angiography; DS, diameter stenosis; FFR, fractional flow reserve; GLPSS, global longitudinal peak systolic strain; IRA, infarct-related artery; LAD, left anterior descending artery; LCx, left circumflex artery; LVEDV, left ventricular end-diastolic volume; LVESV, left ventricular end-systolic volume; LVEF, left ventricular ejection fraction; PCI, percutaneous coronary intervention; PET, positron emission tomography; RCA, right coronary artery; 2VD, two-vessel disease; 3VD, three-vessel disease; NIRA, non-infarct-related artery.

https://doi.org/10.4250/jcvi.2021.0189

Journal of Cardiovascular Imaging JCVI

MBF and oxidative metabolism

NIRAs showed significantly higher stress and resting MBF, MFR, RFR, stress and resting k_{mono}, and their products as compared to IRAs (**Supplementary Table 1**).

Stenotic NIRAs showed significantly lower MFR, RFR, and stress k_{mono} as compared to non-stenotic NIRAs. NIRAs with significant stenosis revealed significantly lower stress MBF, MFR, and RFR as compared to those without. Particularly, RFR > 0.81 could effectively rule out the presence of significant NIRA stenosis (**Figure 2A**). Stress MBF*k_{mono} significantly differed between stenotic vs. non-stenotic NIRAs and between NIRAs with vs. without significant stenosis. Based on the p-values, it was considered that stress k_{mono} mainly contributed to the difference between stenotic vs. non-stenotic NIRAs while stress MBF mainly contributed to the difference between NIRAs with vs. without significant stenosis. However, no significant differences were found for oxidative metabolism parameters themselves between NIRAs with and without significant stenosis (**Table 2**). A representative case is presented in **Figure 3**; the optimal thresholds for the assessment of NIRA stenosis are summarized in **Supplementary Table 2**.

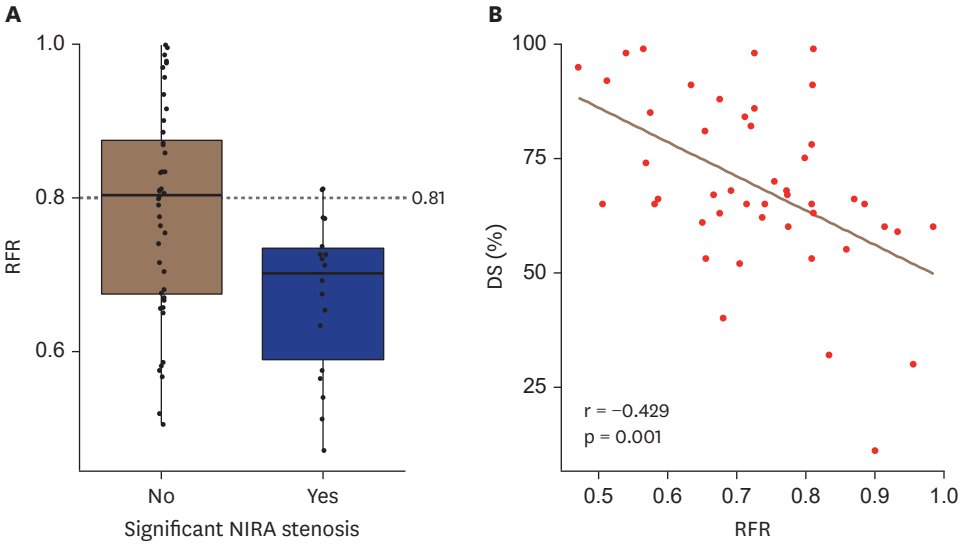

Figure 2. RFR according to the severity of NIRA stenosis. NIRAs with significant stenosis showed significantly lower RFR. RFR > 0.81 could effectively exclude the presence of significant NIRA stenosis (A). Among the PET-derived MBF and oxidative metabolism parameters, RFR shows the best correlation with DS of NIRA (B).
DS, diameter stenosis; NIRA, non-infarct-related artery; RFR, relative flow reserve; PET, positron emission tomography; MBF, myocardial blood flow.

Table 2. Comparison of MBF and oxidative metabolism of non-infarct-related arteries according to stenosis

PET parameters	Stenotic†	Non-stenotic	p	Significant stenosis (+)‡	Significant stenosis (−)	p
Stress MBF (mL/min/g)	1.60 (0.53–3.38)	1.76 (0.70–3.58)	0.095	1.46 (0.64–2.14)	1.71 (0.53–3.58)	0.025*
Resting MBF (mL/min/g)	0.76 (0.41–1.46)	0.74 (0.48–1.24)	0.215	0.75 (0.41–0.96)	0.76 (0.48–1.46)	0.445
MFR	2.10 (0.87–4.09)	2.60 (1.08–4.61)	0.019*	1.86 (0.87–4.09)	2.34 (0.99–4.61)	0.019*
RFR	0.72 ± 0.12	0.82 ± 0.14	0.009*	0.70 ± 0.10	0.80 ± 0.14	0.001*
Stress k_{mono} (/min)	0.052 (0.025–0.076)	0.056 (0.040–0.083)	0.023*	0.047 (0.025–0.068)	0.054 (0.039–0.083)	0.193
Resting k_{mono} (/min)	0.041 (0.018–0.058)	0.045 (0.028–0.066)	0.061	0.041 (0.018–0.057)	0.042 (0.028–0.066)	0.171
OMR	1.25 (0.87–1.74)	1.29 (0.88–1.54)	0.302	1.31 (0.99–1.62)	1.26 (0.87–1.74)	0.634
Stress MBF*k_{mono} (mL/min²/g)	0.081 (0.023–0.202)	0.108 (0.033–0.297)	0.038*	0.066 (0.033–0.137)	0.090 (0.023–0.297)	0.027*
Resting MBF*k_{mono} (mL/min²/g)	0.031 (0.007–0.083)	0.032 (0.014–0.069)	0.685	0.031 (0.007–0.048)	0.031 (0.014–0.083)	0.706

k_{mono}, myocardial oxidative metabolism derived by monoexponential curve fitting; MBF, myocardial blood flow; MFR, myocardial flow reserve (stress myocardial blood flow/resting myocardial blood flow); RFR, relative flow reserve; OMR, oxidative metabolism reserve (stress k_{mono}/resting k_{mono}); DS, diameter stenosis; FFR, fractional flow reserve.
*p < 0.05; †DS ≥ 50%; ‡DS ≥ 70% or FFR ≤ 0.80.

https://doi.org/10.4250/jcvi.2021.0189

Journal of Cardiovascular Imaging JCVI

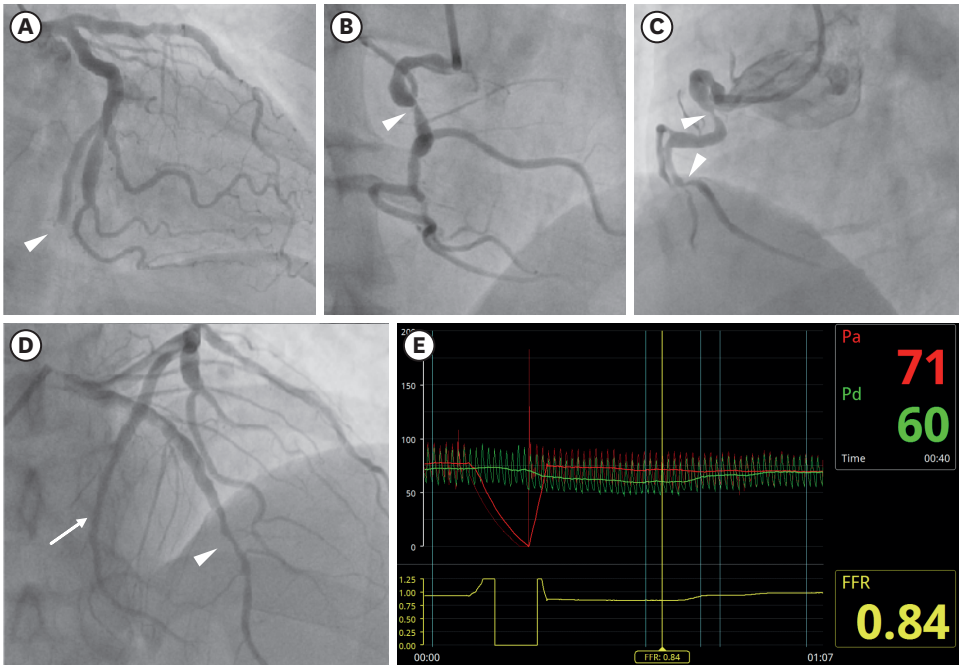

G

Vessel	PET measurements	
LCx (IRA) (after primary PCI)	Stress MBF Rest MBF MFR RFR Stress MBF*k_{mono}	1.49 0.51 2.96 0.56 0.056
RCA (NIRA 1) DS 91%	Stress MBF Rest MBF MFR RFR Stress MBF*k_{mono}	1.69 0.41 4.09 0.63 0.042
LAD (NIRA 2) DS 65% FFR 0.84	Stress MBF Rest MBF MFR RFR Stress MBF*k_{mono}	2.18 0.60 3.18 0.82 0.079

Figure 3. A case of 58-year-old male with STEMI and multivessel disease. The patient underwent primary PCI for the totally occluded LCx (A), which was successfully revascularized (arrow, D). Multifocal significant stenoses were found in mid-RCA (DS up to 91%, arrowheads, B, C). An intermediate stenosis was found in mid-to-distal LAD (DS 65%, arrowhead, D), which was considered non-significant based on its FFR 0.84 (E). RFR was decreased to 0.63 for the RCA while it was preserved > 0.81 for the LAD (F, G).
STEMI, ST-elevation myocardial infarction; PCI, percutaneous coronary intervention; DS, diameter stenosis; RCA, right coronary artery; IRA, infarct-related artery; FFR, fractional flow reserve; LAD, left anterior descending artery; LCx, left circumflex artery; RFR, relative flow reserve; k_{mono}, myocardial oxidative metabolism derived by monoexponential curve fitting; MBF, myocardial blood flow; MFR, myocardial flow reserve; NIRA, non-infarct-related artery.

Modest linear correlations were found for stress MBF (rho = −0.304, p = 0.016), MFR (rho = −0.370, p = 0.004), RFR (r = −0.429, p = 0.001) (**Figure 2B**), stress k_{mono} (rho = −0.303, p = 0.017), resting k_{mono} (rho = −0.274, p = 0.034), and stress MBF*k_{mono} (rho = −0.336, p = 0.008) with DS. In contrast, for the NIRAs with available FFR (n = 25), no significant correlation was found between any of the PET parameters and FFR.

https://doi.org/10.4250/jcvi.2021.0189

Journal of Cardiovascular Imaging JCVI

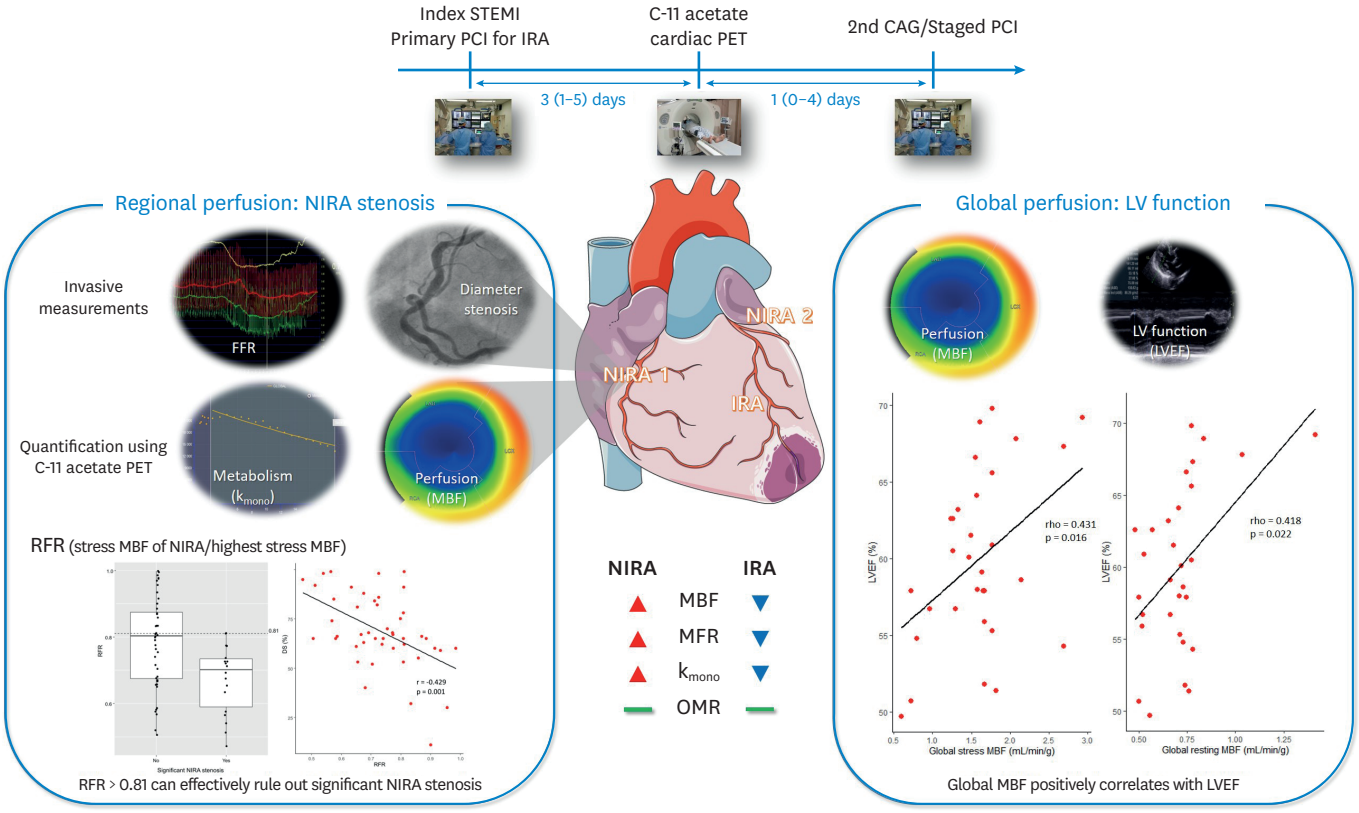

Figure 4. Study workflow and results in summary.
STEMI, ST-elevation myocardial infarction; PCI, percutaneous coronary intervention; IRA, infarct-related artery; CAG, coronary angiography; NIRA, non-infarct-related artery; FFR, fractional flow reserve; PET, positron emission tomography; RFR, relative flow reserve; MBF, myocardial blood flow; MFR, myocardial flow reserve (stress MBF/resting MBF); k_{mono}, myocardial oxidative metabolism derived by monoexponential curve fitting; OMR, oxidative metabolism reserve (stress k_{mono}/resting k_{mono}); LV, left ventricle; LVEF, left ventricular ejection fraction.

Modest, but significant linear correlations were found for global stress MBF (rho = 0.431, p = 0.016), global resting MBF (rho = 0.418, p = 0.022), and stress MBF of the IRA territory (rho = 0.362, p = 0.045) vs. left ventricular ejection fraction (LVEF) while no significant correlation was found for PET parameters vs. diastolic indices.

The **Figure 4** comprehensively summarizes the study workflow and results.

DISCUSSION

The present study evaluated whether MBF and oxidative metabolism quantified by C-11 acetate PET could noninvasively assess NIRA stenosis after primary PCI for STEMI. MBF and oxidative metabolism were significantly higher for NIRAs than IRAs. Among the MBF and oxidative metabolism parameters reflecting the presence and severity of NIRA stenosis, RFR showed the best, but modest correlation with anatomical stenosis severity. It could effectively exclude the presence of significant NIRA stenosis. Global ischemic burden as assessed by stress and rest MBF of the LV correlated with LVEF. To the best of our knowledge, this is the first study to utilize PET for evaluating NIRA stenosis in patients with STEMI.

https://doi.org/10.4250/jcvi.2021.0189

Journal of Cardiovascular Imaging JCVI

To assess the stenotic lesions in NIRA, we took advantage of the C-11 acetate PET, which can quantify both MBF and oxidative metabolism with a single imaging study. C-11 acetate enters the myocardium via the monocarboxylate transporter. The rate of myocardial uptake of C-11 acetate relative to its pooling in the blood correlates with the absolute amount of myocardial perfusion, namely MBF. Compartment modeling of C-11 acetate PET for MBF quantification has been validated.[16] Once in the myocardium, 2 metabolic pathways are present in the metabolism of C-11 acetate. The first one is the slow anabolic pathway, which uses C-11 acetate as a substrate for fatty acid synthesis to produce the cell membrane. It is the biological mechanism for tumor imaging using C-11 acetate PET. The second pathway is the rapid catabolic pathway, in which C-11 acetate is converted to C-11 acetyl-coenzyme A and enters the tricarboxylic acid cycle. Due to the extremely low proliferative potential, the latter is predominant in the myocardium. Through the rapid metabolic cycle, C-11 is eventually excreted as a form of radioactive carbon dioxide within minutes,[19] shaping a decreasing curve following the initial uptake curve (**Figure 1**). By a monoexponential curve fitting from this curve, k_{mono} can be quantified.

As expected, both MBF and k_{mono} were relatively preserved for the NIRA territories than the IRA territories. Such findings can be attributed to myocardial necrosis with or without microvascular damages in the infarcted myocardium, and the reduction of myocardial oxygen consumption caused by acute ischemia.[20][21] However, the relatively preserved MBF and oxidative metabolism in the NIRA territories should not be simply regarded as 'normal'. The MBF measured in the remote myocardium has been reported to be lower than that measured in healthy controls.[22] Our data also revealed variable stress MBF, MFR, and k_{mono} even in the *non-stenotic* NIRA territories, which were frequently lower than the normal ranges reported thus far.[10][23] The remote myocardial tissue shortly (up to 7 days) after successful revascularization for STEMI showed edema, inflammation, fibrosis, and increased interstitial space,[24] which could have affected the PET measures in the present study.

We further tested MBF and oxidative metabolism to differentiate stenotic NIRAs and those with significant stenosis. RFR showed the best correlation with the presence and anatomical severity of NIRA stenosis. Notably, the RFR threshold > 0.81 could be used to exclude the presence of significant NIRA stenosis. RFR reflects the relative decrease in stress MBF in a certain coronary territory. Its decrease specifically indicates the presence of focal coronary stenosis while MBF and MFR are affected by other pathophysiology including microvascular dysfunction and diffuse atherosclerosis.[18] RFR measured with C-11 acetate PET was also useful in detecting focal stenosis in the present study, as it was with other perfusion radiotracers. It could be attributed to its nature of a relative ratio, normalizing the potential discrepancies in MBF values by radiotracers and compartment models.[25] However, its correlation with FFR could not be clarified in our small study population with limited FFR measurements for those having 50–70% DS.

Oxidative metabolism parameters could not differentiate significant NIRA stenosis. It may partly be attributed to the different kinetics of perfusion and metabolism in the setting of acute myocardial ischemia and reperfusion. In experimental models, oxidative metabolism is declined by acute ischemia and is slowly recovered following reperfusion, remaining reduced for a prolonged time.[9][26] Moreover, k_{mono} could have been affected by myocardial work, mechanical stress, and corresponding metabolic adaptation as well as the upfront ischemic burden resulting from the stenotic lesions.[7]

https://doi.org/10.4250/jcvi.2021.0189

Journal of Cardiovascular Imaging JCVI

Gaur et al.[27] utilized cardiac CT-derived FFR to evaluate NIRA stenosis in 60 STEMI patients. It showed an accuracy of 72% and a modest correlation (r = 0.57) against invasive FFR. However, the accuracy was highly subject to volume-to-mass ratio and the radiation exposure was higher than CAG (6.2 ± 1.7 mSv vs. 2.8 ± 1.3 mSv, respectively, p < 0.001), which was apparently higher than that from C-11 acetate PET following our protocol (2.4 ± 0.2 mSv, data not shown). Additional contrast loading for CT angiography is also of concern in such patients. Cardiac magnetic resonance can be another option without radiation hazard. Everaars et al.[28] measured MBF for NIRA territories in 77 patients, showing apparently higher accuracy than Gaur et al.,[27] unaffected by the severity of microvascular dysfunction. However, wide overlaps were shown between stress MBF and MFR of FFR-positive vs. FFR-negative NIRA stenoses, similar to our results. It may be attributed to the remaining diffuse atherosclerosis even after primary PCI[29] which can decrease myocardial perfusion even in the absence of significant stenosis.

Global stress and resting MBF showed positive correlations with LVEF. Our observation suggests the close link between the global ischemic burden remaining after primary PCI for STEMI with systolic LV function, an important indicator of patients' prognosis.[30] Although data are not available for this specific population, future investigations may shed light on the prognostic role of PET in STEMI.

The number of patients included in the present study (n = 31) was less than initially targeted (n = 40). As per the pre-defined study protocol,[14] FFR was indicated only for less than half of the NIRAs which had 50–70% DS, limiting the potential distribution of FFR to a narrow range. Also, the initial screening of eligible patients (STEMI with multivessel disease) and selection of those in need of FFR measurement were based on visual estimation. Despite its ability to exclude the need for additional revascularization for significant NIRA stenosis, the correlation of RFR with DS was only modest and there were substantial overlaps between NIRAs with and without significant stenosis. Therefore, it may be useful in limited cases for which additional invasive procedures are risky or potential benefits are unlikely. Also, the invasive measures for microvascular dysfunction were not available, which could have affected PET indices measured in the NIRA territories. C-11 acetate PET needs an on-site cyclotron, and flexible radioisotope production is required to match the clinical workflow of STEMI. Therefore, we used a one-day rest-stress PET protocol with a single radioisotope production, which takes approximately 90 min per case, for improved clinical feasibility.

In conclusion, RFR measured by C-11 acetate PET could be used for the assessment of NIRAs in patients with STEMI and multivessel disease and may reduce unnecessary staged procedures.

SUPPLEMENTARY MATERIALS

Supplementary Table 1

Global and regional measurements of MBF and oxidative metabolism in study patients

Click here to view

Supplementary Table 2

Optimal thresholds and diagnostic performances of PET parameters in detecting NIRA stenosis

Click here to view

https://doi.org/10.4250/jcvi.2021.0189

Journal of Cardiovascular Imaging JCVI

Supplementary Figure 1

Standardized 17-segment model for territory-based measurements of myocardial blood flow and oxidative metabolism. The standardized 17-segment model (left) shows the segment numbers given in a numerical order starting from the basal anterior segment (segment 1) to apex (segment 17). The image on the right shows the conventional assignment of the coronary territories based on the 17-segment model. LAD territory correlates to the sum of the segments 1, 2, 7, 8, 13, 14, and 17; LCx territory to the segments 5, 6, 11, 12, and 16; and RCA territory to the segments 3, 4, 9, 10, and 15.

Click here to view

REFERENCES

1. Kim Y, Ahn Y, Cho MC, Kim CJ, Kim YJ, Jeong MH. Current status of acute myocardial infarction in Korea. *Korean J Intern Med* 2019;34:1-10.
PUBMED | CROSSREF
2. Sorajja P, Gersh BJ, Cox DA, et al. Impact of multivessel disease on reperfusion success and clinical outcomes in patients undergoing primary percutaneous coronary intervention for acute myocardial infarction. *Eur Heart J* 2007;28:1709-16.
PUBMED | CROSSREF
3. Writing Committee MembersLawton JS, Tamis-Holland JE, et al. 2021 ACC/AHA/SCAI guideline for coronary artery revascularization: a report of the American College of Cardiology/American Heart Association joint committee on clinical practice guidelines. *J Am Coll Cardiol* 2022;79:e21-129.
PUBMED | CROSSREF
4. Tavakol M, Ashraf S, Brener SJ. Risks and complications of coronary angiography: a comprehensive review. *Glob J Health Sci* 2012;4:65-93.
PUBMED | CROSSREF
5. Hanratty CG, Koyama Y, Rasmussen HH, Nelson GI, Hansen PS, Ward MR. Exaggeration of nonculprit stenosis severity during acute myocardial infarction: implications for immediate multivessel revascularization. *J Am Coll Cardiol* 2002;40:911-6.
PUBMED | CROSSREF
6. Thim T, van der Hoeven NW, Musto C, et al. Evaluation and management of nonculprit lesions in STEMI. *JACC Cardiovasc Interv* 2020;13:1145-54.
PUBMED | CROSSREF
7. Knaapen P, Germans T, Knuuti J, et al. Myocardial energetics and efficiency: current status of the noninvasive approach. *Circulation* 2007;115:918-27.
PUBMED | CROSSREF
8. Sörensen J, Harms HJ, Aalen JM, Baron T, Smiseth OA, Flachskampf FA. Myocardial efficiency: a fundamental physiological concept on the verge of clinical impact. *JACC Cardiovasc Imaging* 2020;13:1564-76.
PUBMED | CROSSREF
9. Naya M, Tamaki N. Imaging of myocardial oxidative metabolism in heart failure. *Curr Cardiovasc Imaging Rep* 2014;7:9244.
PUBMED | CROSSREF
10. Duvernoy CS, Raffel DM, Swanson SD, et al. Left ventricular metabolism, function, and sympathetic innervation in men and women with type 1 diabetes. *J Nucl Cardiol* 2016;23:960-9.
PUBMED | CROSSREF
11. Güçlü A, Knaapen P, Harms HJ, et al. Disease stage-dependent changes in cardiac contractile performance and oxygen utilization underlie reduced myocardial efficiency in human inherited hypertrophic cardiomyopathy. *Circ Cardiovasc Imaging* 2017;10:e005604.
PUBMED | CROSSREF
12. Liu S, Lin X, Shi X, et al. Myocardial tissue and metabolism characterization in men with alcohol consumption by cardiovascular magnetic resonance and 11C-acetate PET/CT. *J Cardiovasc Magn Reson* 2020;22:23.
PUBMED | CROSSREF

13. Kim MC, Bae S, Ahn Y, et al. Benefit of a staged in-hospital revascularization strategy in hemodynamically stable patients with ST-segment elevation myocardial infarction and multivessel disease: analyses by risk stratification. *Catheter Cardiovasc Interv* 2021;97:1151-9.
PUBMED | CROSSREF

14. Kim MC. Timing of FFR-guided PCI for non-IRA in STEMI and MVD (OPTION-STEMI) [Internet]. Bethesda, MD: U.S. National Library of Medicine; 2020 [cited 2021 Sep 2]. Available at: https://clinicaltrials.gov/ct2/show/NCT04626882.

15. Wu YW, Naya M, Tsukamoto T, et al. Heterogeneous reduction of myocardial oxidative metabolism in patients with ischemic and dilated cardiomyopathy using C-11 acetate PET. *Circ J* 2008;72:786-92.
PUBMED | CROSSREF

16. van den Hoff J, Burchert W, Börner AR, et al. [1-^{11}C]Acetate as a quantitative perfusion tracer in myocardial PET. *J Nucl Med* 2001;42:1174-82.
PUBMED

17. Cerqueira MD, Weissman NJ, Dilsizian V, et al. Standardized myocardial segmentation and nomenclature for tomographic imaging of the heart. A statement for healthcare professionals from the Cardiac Imaging Committee of the Council on Clinical Cardiology of the American Heart Association. *Circulation* 2002;105:539-42.
PUBMED | CROSSREF

18. Cho SG, Park KS, Kim J, et al. Coronary flow reserve and relative flow reserve measured by N-13 ammonia PET for characterization of coronary artery disease. *Ann Nucl Med* 2017;31:144-52.
PUBMED | CROSSREF

19. Plathow C, Weber WA. Tumor cell metabolism imaging. *J Nucl Med* 2008;49 Suppl 2:43S-63S.
PUBMED | CROSSREF

20. Kalff V, Hicks RJ, Hutchins G, Topol E, Schwaiger M. Use of carbon-11 acetate and dynamic positron emission tomography to assess regional myocardial oxygen consumption in patients with acute myocardial infarction receiving thrombolysis or coronary angioplasty. *Am J Cardiol* 1993;71:529-35.
PUBMED | CROSSREF

21. Schulz R, Kappeler C, Coenen H, Bockisch A, Heusch G. Positron emission tomography analysis of [1-^{11}C] acetate kinetics in short-term hibernating myocardium. *Circulation* 1998;97:1009-16.
PUBMED | CROSSREF

22. Kaufmann PA, Camici PG. Myocardial blood flow measurement by PET: technical aspects and clinical applications. *J Nucl Med* 2005;46:75-88.
PUBMED

23. Murthy VL, Bateman TM, Beanlands RS, et al. Clinical quantification of myocardial blood flow using PET: joint position paper of the SNMMI cardiovascular council and the ASNC. *J Nucl Med* 2018;59:273-93.
PUBMED | CROSSREF

24. Biesbroek PS, Amier RP, Teunissen PF, et al. Changes in remote myocardial tissue after acute myocardial infarction and its relation to cardiac remodeling: a CMR T1 mapping study. *PLoS One* 2017;12:e0180115.
PUBMED | CROSSREF

25. Nesterov SV, Deshayes E, Sciagrà R, et al. Quantification of myocardial blood flow in absolute terms using ^{82}Rb PET imaging: the RUBY-10 Study. *JACC Cardiovasc Imaging* 2014;7:1119-27.
PUBMED | CROSSREF

26. Heyndrickx GR, Wijns W, Vogelaers D, et al. Recovery of regional contractile function and oxidative metabolism in stunned myocardium induced by 1-hour circumflex coronary artery stenosis in chronically instrumented dogs. *Circ Res* 1993;72:901-13.
PUBMED | CROSSREF

27. Gaur S, Taylor CA, Jensen JM, et al. FFR derived from coronary CT angiography in nonculprit lesions of patients with recent STEMI. *JACC Cardiovasc Imaging* 2017;10:424-33.
PUBMED | CROSSREF

28. Everaars H, van der Hoeven NW, Janssens GN, et al. Cardiac magnetic resonance for evaluating nonculprit lesions after myocardial infarction: comparison with fractional flow reserve. *JACC Cardiovasc Imaging* 2020;13:715-28.
PUBMED | CROSSREF

29. Gould KL, Johnson NP. Coronary blood flow after acute MI: alternative truths. *JACC Cardiovasc Interv* 2016;9:614-7.
PUBMED | CROSSREF

30. Ng VG, Lansky AJ, Meller S, et al. The prognostic importance of left ventricular function in patients with ST-segment elevation myocardial infarction: the HORIZONS-AMI trial. *Eur Heart J Acute Cardiovasc Care* 2014;3:67-77.
PUBMED | CROSSREF